# Effects of Applied Voltage and Concentration of Chemical Solution on the Electro-osmotic Consolidation of Kaolin

*Wugang Li*[*], *Wenhua Liu, Meilan Shen, Xiuli Sun, Zhihua Li*

Jiangnan University, Wuxi, 214122, China.
[*]E-mail: Liwugangdlut@163.com

Electro-osmotic chemical technique is an effective method to reinforce soft clay. In this study, a series of electro-osmotic chemical tests were conducted on kaolin to investigate the effects of applied voltage and concentration of chemical solution on the shear strength. The changes in various factors, such as current, electrical potential, settlement, and drainage volume during the tests were analyzed. The cohesion and internal friction angle of the treated slurry were calculated using the values of variables monitored during the experiments. The shear strength after treatment was measured to obtain the efficiency for the electro-osmotic chemical technique. The experimental data indicated that the higher applied voltage reduced the economic effectiveness of electro-osmotic chemical treatment (ECT). However, the higher concentration of injected solution promoted the consolidation of kaolin and had only a slight impact on the economic effectiveness of ECT. Besides, the values of cohesion and internal friction angle of the treated sample increased with the increase in applied voltage and the concentration of chemical solution. The results of this study provide some references for seeking a better curing scheme for the electro-osmotic chemical treatment in future engineering applications.

**Keyword:** Soft soil, Electro-osmosis, Chemical solution, Shear strength, Consolidation

## 1. INTRODUCTION

Electro-osmotic is one of the most effective technologies for treating soft clay. After Casagrande [1] successfully applied electro-osmotic technology to reinforce the soft soils for the first time, the technology has been applied to many different geotechnical problems. Lamont-Black et al. [2] applied the electro-osmosis consolidation method to strengthen the embankment and achieved a 25% in cost reduction compared to using the conventional soil nails. Ling et al. [3] used electroosmosis method to dewater the pavement subgrade soil. Zou et al. [4] adopted electrically conductive wick drain and automated power supply to consolidate marine hydraulically-filled sludge ground. In recent years,

*Int. J. Electrochem. Sci.,* 16 (**2021**) Article Number: 211215

2

chemical solutions are injected to soft soils during electro-osmotic process to improve the efficiency of the process and the strengthen the soft soils. Ou et al. [5] injected calcium chloride and sodium silicate solutions into a Taipei field test site during electroosmosis and found that the shear strength of the soil surrounding the anodes increased significantly. Zhang et al. [6] injected calcium chloride, sodium carbonate and alum solutions into marine soils during electro-osmotic in a field study and found that the bearing capacities of the soils increased quickly with time. These studies have shown that the electro-osmotic chemical treatment (ECT) is a promising and useful method for reinforcing the shear strength of soft soils.

The ECT method requires chemical solutions at cathodic or anodic regions. Recently, many researchers have tried different kinds of chemical solutions to seek a better scheme of electro-osmotic chemical treatment. Mohamedelhassan and Shang [7] compared the curing effect of injecting the calcium chloride and aluminum sulfate solutions into an offshore calcareous soil. The results indicated that the calcium chloride solution was better than the aluminum sulfate solution due to a faster transport rate of $Ca^{2+}$ than that of $Al^{3+}$. Otsuki et al. [8] improved the shear strength of kaolin soil at the region near the cathode up to 300 kPa by using 2 mol/L $Mg(CH_3COO)_2$ solution as the anolyte solution and 2 mol/L $Na_2CO_3$ solution as the catholyte solution. However, the region near the anode lacked improvement. Keykha et al. [9] injected $CaCl_2$ into the anode and a blend of bacteria and urea solution that released high concentrations of carbonate into the cathode. During the treatment, $CaCO_3$ was precipitated out and increased the shear strength of soft soils. Chang et al. [10] used calcium chloride solution as the injection material, studied the effectiveness of ECT, and reported a significant increase in the shear strength of kaolin near the cathode that indicated that pozzolanic reaction occurred during the treatment. Chien et al. [11] injected $CaCl_2$ and $Na_2SiO_3$ solutions into silty clay from the anode and a relay pipe. Some silicate ion reacted with calcium, and resulted in the cementing agent, which improved the shear strength of silty clay. Xue et al. [12] studied the mechanism of clay reinforcement using electro-osmotic chemicals.

Some studies have focused on the shear strength [13-15] and variations in the fabric of the treated soil [16-19]. However, only a handful of studies have evaluated the effects of concentration of injected solution and applied voltages on the cohesion and friction angle of the treated soils. In previous studies, $CaCl_2$ [9, 20] and $Na_2SiO_3$ [21] have often been used as the anolyte and catholyte ionic solutions, respectively. The current study used $CaCl_2$ solution (as the anolyte) and the mixed $Na_2SiO_3$ and NaOH solutions (as the catholyte) to improve the soft clay. During the treatment, various factors, such as current, settlement and drainage volume were monitored to explore the mechanism of ECT. Variations in the shear strength and the fabric of the treated soil after treatment were investigated to evaluate the effectiveness of ECT. The results of this study provide some references for seeking a better curing scheme for the electro-osmotic chemical treatment in future engineering applications.

## 2. MATERIAL AND METHODS

### 2.1 Soil description

The soil used in the current study was kaolin, which was purchased from Hengyuan New Material Co., Ltd. The kaolin was in the form of powder and the initial water content was about 0.1%. The liquid

and plastic limits of the kaolin were 49% and 15%, respectively. The chemical composition was determined using XRF (X-ray fluorescence spectroscopy). The dominant components of the kaolin were silicon oxide and aluminium oxide with concentrations of 51.41% and 26.3% by weight, respectively. The physical properties and the chemical composition of kaolin are presented in Table 1.

**Table 1.** Physical properties and chemical composition of kaolin

| Geotechnical properties | |
|---|---|
| Specific gravity | 2.72 |
| Plastic limit, PL (%) | 15 |
| Liquid limit, LL, (%) | 49 |
| Plasticity index | 34 |
| Chemical composition (weight proportion, %) | |
| $SiO_2$ | 51.41 |
| $Al_2O_3$ | 47.06 |
| $Fe_2O_3$ | 0.36 |
| CaO | 0.24 |
| MgO | 0.21 |
| $TiO_2$ | 0.5 |
| $Ka_2O$ | 0.1 |
| $Na_2O$ | 0.12 |

*2.2 Apparatus*

For a comprehensive study of the influence of voltage and solution concentration on ECT, an electro-osmotic device was designed as shown in Figure 1. The electro-osmotic cell was made up of plexiglass and divided into three chambers. The main cell had internal dimensions of $260 \times 150 \times 200 mm^3$. The anode and cathode chambers with the internal dimensions of $50 \times 150 \times 200 mm^3$ were used to inject the chemical solutions and drain fluid. A power supply was connected to the electrodes (MMO Ti), which were inserted in the solutions contained in the anode and cathode chambers. A current collector was also connected to the electrodes to record the changes in current during ECT. In addition, there were five holes in the wall of the main cell, which were used to measure the electrical potential during ECT. Five voltage probes (V1, V2, V3, V4, and V5) were inserted into the kaolin through the holes on the wall of main cell. The distances from V1, V2, V3, V4, and V5 to anode were 10 mm, 70 mm, 130 mm, 190 mm, and 250 mm, respectively. The V1 and V5 were close to the electrodes to measure the voltage loss between the kaolin and electrodes. The voltages at V1, V2, V3, V4, and V5 were measured using a voltage collector to determine the distribution of the electrical potential during the experiment. A 20 mm thick plate on the top of slurry was used to apply the load. A settlement sensor was placed on the plate so that the settlement of the sample could be measured during ECT. Two spillway holes, one on the wall of the anode chamber and the other on the cathode chamber, were used to drain the discharge fluid during ECT. The volume of the discharge fluid from the cathode cell was collected and recorded using a measuring cylinder, as shown in Figure 1. At the end of the ECT, samples from different locations of

the treated slurry were taken. The treated sample was dried to determine the water content. The shear strength of the treated sample was determined using a triaxial apparatus.
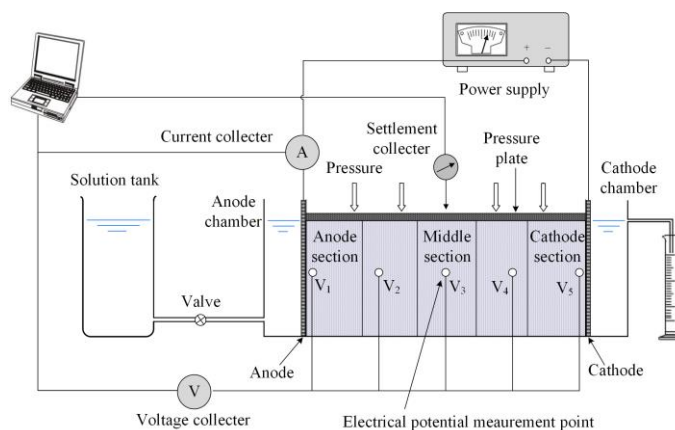


**Figure 1**. Electro-osmotic experiment system

*2.3 Test procedure*

The electro-osmotic chemical experiment procedures are as follows:

1. Deionized water was added to kaolin to obtain a slurry sample with an initial moisture content of 49% (equal to the liquid limit).

2. Vaseline was smeared on the inner surface to decrease the frictional force between the slurry sample and the wall of the cell.

3. Two filter papers were placed on the gates to avoid the leakage of the slurry sample.

4. The slurry was poured into the electro-osmotic cell. Then a vibrator was inserted into the slurry to expel air from the sample.

5. A pressure plate was placed at the top of the slurry sample. A load of 10 kPa was applied on the pressure plate for 10 h.

6. The chemical solutions used in this experiment are $CaCl_2$ solution and the mixed NaOH and $Na_2SiO_3$ solution. The concentrations of the chemical solutions for different applied voltage are listed in Table 2. The $CaCl_2$ solution was poured into the anode cell, and the mixed NaOH and $Na_2SiO_3$ solution was poured into the cathode cells.

7. Voltage was applied on the slurry sample using a power supply after the electrodes were inserted in the solutions. After providing power for 48h, the $CaCl_2$ solution was removed from the anode chamber after the power supply was turned on for 48 h. The total duration of ECT was 72 h.

8. During the electro-osmotic experiment, the current ($I$), settlement ($y$), electrical potential ($\phi$), and drainage volume ($q$) were monitored. After the experiments, the water content ($w$) of the slurry sample was successively measured at the distances of 1 cm, 7 cm, 13 cm, 19 cm, and 25 cm to the anode. Meanwhile, the shear strengths ($\tau_f$) at the anode, middle, and cathode sections of the sample were determined using a triaxial apparatus.

**Table 2.** Schema of the electro-osmotic chemical experiment

| Test No. | Applied Voltage (V) | Electric potential gradient (V/cm) | $CaCl_2$ (mol/L) | $Na_2SiO_3$ (mol/L) | NaOH (mol/L) |
|---|---|---|---|---|---|
| EC_0.1_0.5 | 13 | 0.5 | 0.1 | 0.05 | 0.05 |
| EC_0.1_1.0 | 26 | 1.0 | 0.1 | 0.05 | 0.05 |
| EC_0.1_1.5 | 39 | 1.5 | 0.1 | 0.05 | 0.05 |
| EC_0.5_0.5 | 13 | 0.5 | 0.5 | 0.25 | 0.25 |
| EC_0.5_1.0 | 26 | 1.0 | 0.5 | 0.25 | 0.25 |
| EC_0.5_1.5 | 39 | 1.5 | 0.5 | 0.25 | 0.25 |
| EC_1.0_0.5 | 13 | 0.5 | 1.0 | 0.5 | 0.5 |
| EC_1.0_1.0 | 26 | 1.0 | 1.0 | 0.5 | 0.5 |
| EC_1.0_1.5 | 39 | 1.5 | 1.0 | 0.5 | 0.5 |

## 3. RESULTS AND DISCUSSION

### 3.1 Effect of applied voltage and concentration of chemical solution on current

The variation of the current on the whole process is presented in Figure 2. The slurry samples had the same initial water content, which means that the samples had the same initial soil resistance. Therefore, the initial currents increased with the increase in voltage. As the experiment went on, the soil resistance increased rapidly due to the significant decline in water content in the first 32 h (shown in Figure 3). Due to this reason, the current decreased rapidly with time. Then, the current decreased to reach a stable value at the end of experiments. The shape of the current-time curves in Figure 2 is similar with Cameselle and Reddy [22]. The current during the electro-osmotic chemical treatment was induced by the ionic electro-migration and ionic diffusion and can be expressed by Equation (1).

$$I = -\sigma^* \frac{\partial \phi}{\partial x} - \sum FD_i^e \frac{\partial c_i}{\partial x} \qquad (1)$$

where $\sigma^*$ is the effective electrical conductivity, $\phi$ is the electrical potential, $x$ is the distance from cathode, $F$ is the Faraday's constant, $D_i^e$ is the effective diffusion coefficient of ion i, and $c_i$ is the concentration of ion i. The second term on the right-hand side of Equation (1) can be neglected because the ionic diffusion is very weak in kaolin with low permeability. Therefore, the current during electro-osmotic process was determined by the applied voltage and $\sigma^*$, which can be determined by Equation (2).

$$\sigma^* = F \sum z_i u_i^e c_i \qquad (2)$$

where $z_i$ is the charge of ion i, and $u_i^e$ is the effective ionic mobility of ion i, which can be expressed using Equation (3).

$$u_i^e = u_i \tau n \qquad (3)$$

where $u_i$ is the ionic mobility, $\tau$ is the tortuosity, and $n$ is the porosity. The slurry with the same concentration of injected chemical solution had the same effective ionic mobility. When the experiment started, $Ca^{2+}$ migrated to the slurry from the anode chamber due to the electroosmosis and electron migration. Meanwhile, both the $OH^-$ and $SiO_3^{2-}$ migrated to the slurry from the cathode chamber. This led to an increase in the ionic concentration in the pore water. Therefore, the effective electrical

conductivity increased with the concentration of the injected chemical solution according to Equation (2). With the increase of effective electrical conductivity, the current increased with the increase of concentration of the injected chemical solution under the same applied voltage at the initial stage, as shown in Figure 2. The average water content and the porosity decreased as the experiment proceeded. This led to the decrease of the effective ionic mobility. At the end of the ECT, the current decreased to a stable value as shown in Figure 2. The stable values of current for various samples differed from each other, which was, due to the different applied voltages and concentrations of injected solution.



(a) 13 V applied voltage          (b) 26 V applied voltage          (c) 39 V applied voltage
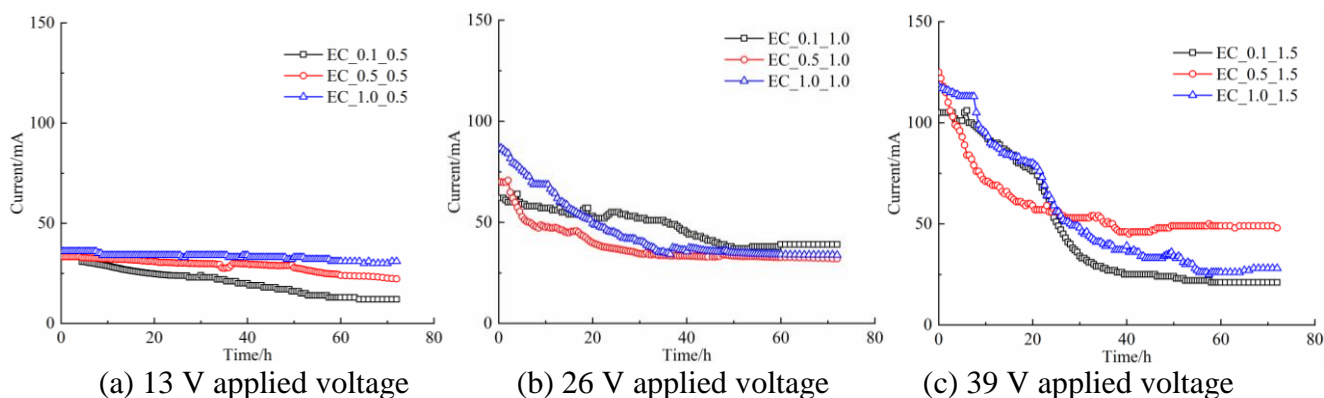
**Figure 2**. Relationship between the current and time under different applied voltages and concentrations of injected solutions

*3.2 Effect of applied voltage and concentration of chemical solution on drainage volume*

The flow rate during the electro-osmotic process can be expressed by Equation (4).

$$q = -\left(k_h \frac{\partial h}{\partial x} + k_e \frac{\partial \phi}{\partial x}\right)A = -\left(k_h \frac{\partial h}{\partial x} + \frac{n\varepsilon_w \varphi_z}{\eta} \frac{\partial \phi}{\partial x}\right)A \qquad (4)$$

where $q$ is the total flow rate, $k_h$ is the hydraulic permeability coefficient, $h$ is the hydraulic head, $k_e$ is the electro-osmotic permeability, $n$ is the porosity of the sample, $\varepsilon_w$ is the permittivity of the pore water, $\varphi_z$ is the zeta potential, and $\eta$ is the viscosity of the pore water. The hydraulic permeability coefficient $k_h$ is very low compared to the electro-osmotic permeability $k_e$ in kaolin. Therefore, the first term of the right-hand side of Equation (4) can be neglected. As seen from Equation (4), higher electrical potential gradient leads to faster flow rate. Due to this reason, the slurry sample with the same chemical solutions will discharge more fluid if a larger electrical potential is applied to the sample, as shown in Figure 3.

Due to the effects of electro-osmotic and electron migration process, $Ca^{2+}$, $OH^-$ and $SiO_3^{2-}$ migrated into the slurry sample during the experiment. The permittivity and viscosity of the pore water can be assumed constant within fairly large ranges of electrolyte concentrations. The increment of ionic concentrations in the pore water decreases the thickness of the electrical double layer. This means that the effective porosity of the slurry sample increases with the increase in the chemical solutions. This leads to the increase of electro-osmotic permeability. On the contrary, the zeta potential $\varphi_z$ usually decreases with the increase in the concentration of chemical solutions [23]. It leads to the decrease of

electro-osmotic permeability $k_e$. The electro-osmotic permeability $k_e$ depends on the combined effects of the effective porosity and the zeta potential. Mohamedelhassan and Shang [24] have pointed out that the electro-osmotic permeability is usually controlled by the effective porosity at low concentrations of the chemical solutions. Therefore, the drainage volume increased with the increase of concentration of the chemical solutions, as shown in Figure 3.
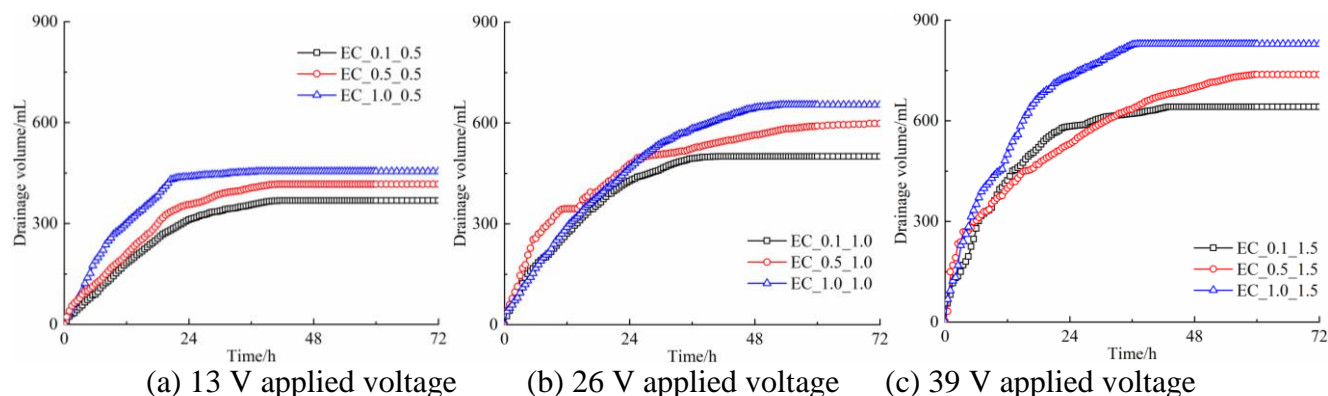


(a) 13 V applied voltage    (b) 26 V applied voltage    (c) 39 V applied voltage

**Figure 3**. Relationship between the drainage volume and time under different applied voltages and concentration of injected solutions

### 3.3 Effect of applied voltage and concentration of chemical solution on settlement

The settlement of the slurry sample during the electro-osmotic experiment is presented in Figure 4. It can be seen that the settlement increased with the increase of voltage and the concentration of solution. The development of settlement with different applied voltages is consistent with Gargano et al. [25]. The coupled effects of applied voltage and concentration of solution on settlement can be explained as follows. The settlement of the slurry sample is related with the consolidation pressure, which can be expressed by Equation (5) in this study.

$$p' = p - u_w \tag{5}$$

where $p'$ is the effective pressure, $p$ is the external pressure, and $u_w$ is the pore water pressure. The pore water pressure can be determined by the mass conservation law, expressed using Equation (6).

$$\frac{\partial(\rho n)}{\partial t} = \frac{\partial}{\partial x}\left(\rho \frac{k_h}{\eta}\frac{\partial u_w}{\partial x} + \rho k_e \frac{\partial \phi}{\partial x}\right) \tag{6}$$

where $\rho$ is the density of the pore fluid. The boundary condition states that the pore water pressures at the anode and cathode become zero before the $CaCl_2$ solution is removed from the anode chamber. Then, the pore water pressure can be obtained from Equation (6) and expressed as Equation (7).

$$u_w(x,t) = \frac{\eta}{k_h}\left(\int_0^x k_e dx - \frac{x}{l}\int_0^l k_e dx\right)\frac{\partial \phi}{\partial x} \tag{7}$$

where $x$ is the distance from the cathode, $t$ is the duration of the electro-osmotic experiment. Equation (7) indicates that the pore water pressure is determined by the electro-osmotic permeability $k_e$

and the gradient of electrical potential $\frac{\partial \phi}{\partial x}$. Beddiar et al. [26] reported that the electro-osmotic permeability $k_e$ of kaolin was pH-dependent and increased with the increase of pH value. Therefore, the electro-osmotic permeability $k_e$ can be written as: $k_e = k_e\left(pH(x,t)\right)$. Moreover, higher concentrations of injected solutions in the cathode chamber led to a higher pH value of the slurry samples. Therefore, the development of negative pore water pressure was promoted by the difference in the electro-osmotic permeability $k_e\left(pH(x,t)\right)$ and a larger gradient of electrical potential $\frac{\partial \phi}{\partial x}$. According to Equation (5), the effective stress of the slurry sample with higher concentration of the solution and applied voltage was larger than that of the slurry sample with a lower concentration of the solution and applied voltage. Therefore, the settlement of samples with higher concentrations of solution and applied voltage was larger than that with the lower concentrations of the solution, as shown in Figure 4.
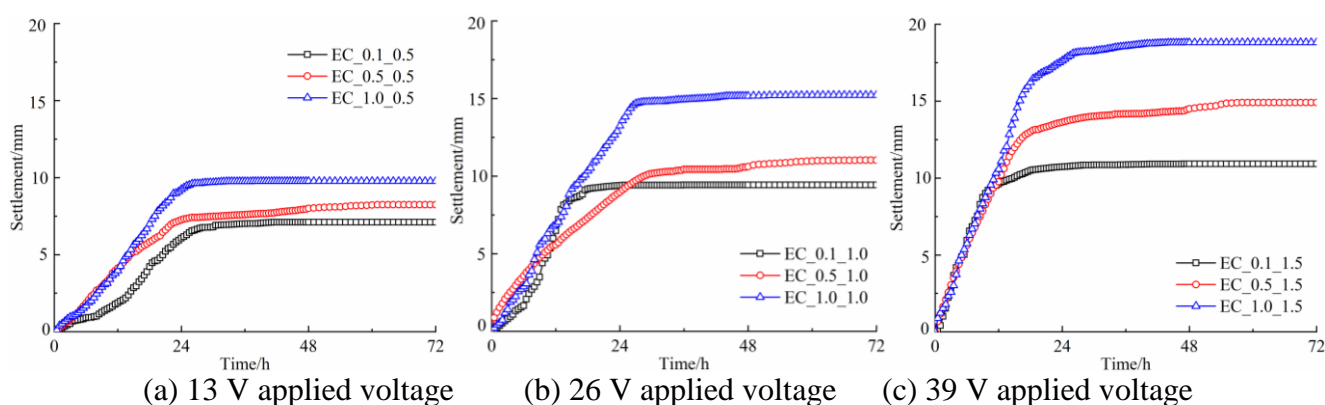


(a) 13 V applied voltage     (b) 26 V applied voltage     (c) 39 V applied voltage

**Figure 4**. Relationship between the settlement and time under different applied voltages and concentration of injected solutions

*3.4 Effect of applied voltage and concentration of chemical solution on distribution of the electrical potential*

The distributions of electrical potential for various the slurry samples at the beginning and the end of ECT are shown in Figure 5. The resistance of the sample is distributed uniformly at the beginning of the experiment. Due to this reason, a linear distribution of electrical potential at the beginning of the experiment was observed. As the experiment went on, $Ca^{2+}$ migrated towards the cathode and $SiO_3^{2-}$ and $OH^-$ migrated towards the anode. The increase in the ionic content of the sample led to the increase of electrical conductivity at the electrodes. However, the distribution of electrical conductivity changed dramatically around the middle section. It can be interpreted by the chemical reactions during the treatment. Anions and cations migrated to the anode and cathode, respectively, during which, certain chemical reactions happened in the slurry sample, as given by Equation (8).

$$Ca^{2+} + 2OH^- = Ca(OH)_2$$
$$Ca^{2+} + 2OH^- + SiO_2 \rightarrow CSH \qquad (8)$$
$$Ca^{2+} + SiO_3^{2-} = CaSiO_3 \downarrow$$
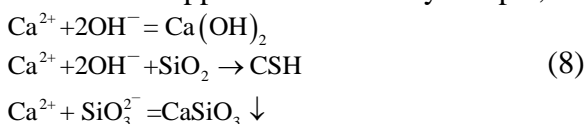
The reaction products cemented the soil particles and blocked the pore channels, leading to the decrease of electrical conductivity around the middle section of the sample. Therefore, the distribution of electrical conductivity changed dramatically as shown in Figure 5. The distributions of electrical potential for various slurry samples under 13 and 26 V applied voltage were similar with Xue et al. [12]. But a great difference was observed under 39 V applied voltage. This may be due to more reaction products being generated at higher applied voltage.
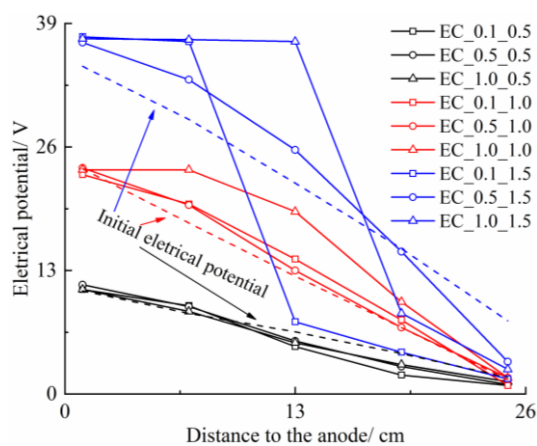


**Figure 5**. Electrical potential distributions at the beginning and the end of ECT

*3.5 Effect of applied voltage and concentration of chemical solution on power consumption*

The economic efficiency of electro-osmotic treatment under different applied voltages and concentrations of injected solution is evaluated in this section. The energy consumption during ECT is given by Equation (9).

$$E=\int_0^t UI(t)\mathrm{d}t \qquad (9)$$

where $E$ is the energy consumption during ECT, $U$ is the applied voltage, and $I(t)$ is the current value at a certain time $t$. The relationship between the energy consumption and the settlement is presented in Figure 6. It can be seen that the energy consumption increased with the increase in applied voltage under the same settlement during the treatment. It was because, at a higher applied voltage, a higher proportion of energy was consumed to generate heat in the slurry sample. This means that the economic effectiveness of ECT decreased with the increase in applied voltage. Interestingly, Figure 6 shows that, under the same voltage, the energy consumption-settlement curves were almost identical before the settlement increased to reach a stable value. A similar phenomenon was observed in some previous works [14, 27-28]. The experimental results suggested that the effectiveness and efficiency of ECT can be improved at lower applied voltages and higher concentrations of injected solution.
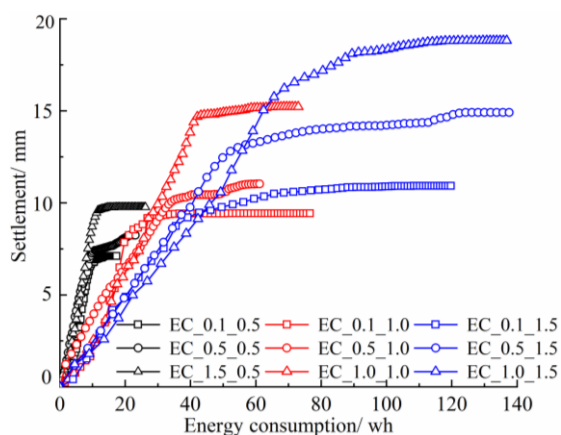
**Figure 6**. Relationship between the settlement and energy consumption under different applied voltages and concentration of injected solutions

*3.6 Effect of applied voltage and concentration of chemical solution on water content and unconfined shear strength*

The effective stress increased due to the negative pore water pressure according to the effective stress principle, thereby causing consolidation of the slurry sample. The water content of the slurry sample decreased due to consolidation, indicating that the water content had a positive correlation with the negative pore water pressure. In other words, the decrease in water content was induced by the increase in the absolute value of the negative pore water. The $CaCl_2$ solution was removed from the anode chamber, which induced the increase in absolute value of the negative pore water pressure. Therefore, the water content decreased from cathode to anode, as shown in Figure 7. To be specific, the water content at 25 cm from anode was 2.1 %-6.8 % higher than that at 1 cm from anode.

The relationship between the unconfined shear strength and water content after treatment is shown in Figure 8. The initial unconfined shear strength of the slurry sample was about 0 kPa. The increase in unconfined shear strength increased from 11 kPa / 24h to 28 kPa / 24h during the treatment. The maximum and minimum unconfined shear strengths after the treatment were 32 kPa (under 13V voltage and 0.1 mol/L $CaCl_2$ solution) and 84 kPa (under 39V voltage and 1 mol/L $CaCl_2$ solution), respectively. The experiment results demonstrated that the ECT technique is an effective method for improving the strength of kaolin. The applied voltage and concentration of the injected solution obviously influences improvements of soil strength. Zhang et al. [6], Ou [29] and Chang et al. [30] obtained the similar conclusion by injecting saline solution into soil. A nonlinear expression, as shown in Figure 8, was used to describe the relationship between the unconfined shear strength and the water content. The unconfined shear strength originated from the reduction of water content and the cementation generated by the chemical reaction. Therefore, the experimental data of the treated sample with lower concentration of injected solution was more likely to be located below the fitting curve. On the other hand, the experimental data of the treated sample with higher concentration of injected solution was more likely to be located above the fitting curve.
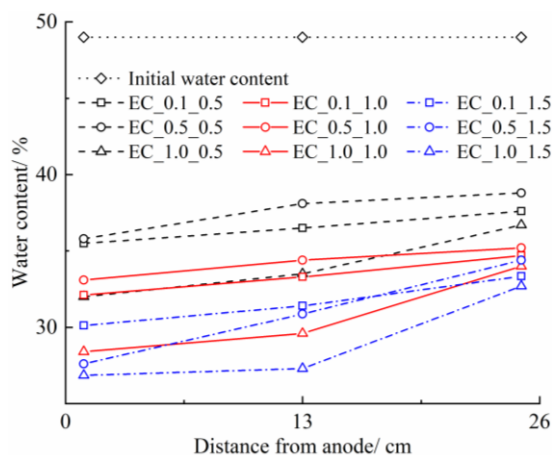
**Figure 7**. Distributions of water content for different applied voltages and concentration of injected solutions
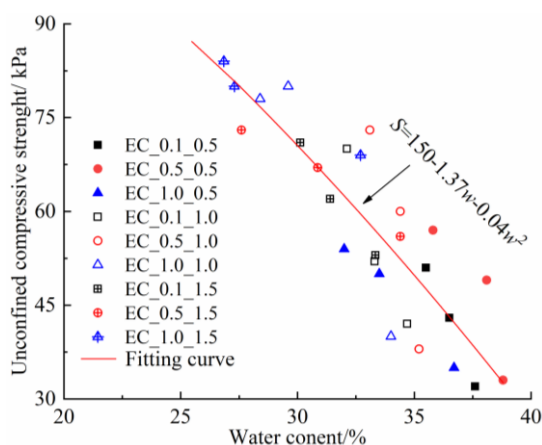


**Figure 8**. Relationship between the unconfined shear strength and water content

*3.7 Effect of applied voltage and concentration of chemical solution on cohesion and frictional angle*

Mohr-Coulomb criterion is widely used in geotechnical engineering to access the safety and stability of civil structures. The salinity of the pore fluid has been shown to have a significant influence on the shear strength of soils [16, 31-32]. The shear strength of treated samples was affected by the thickness of the double layer, which is determined by the salinity of pore fluid. In addition, it is also known that the shear strength of a soil depends on the bonding between the soil particles. The cementation generated by the chemical reaction (given by Equation (8)) enhances the bonding between the soil particles. Therefore, it is important to evaluate the change of cohesion and friction angle due to the electro-osmotic chemical treatment. The samples were collected near the anode, cathode and middle sections, and saturated before testing the shear strength. Triaxial compression tests under the action of lateral pressures of 50 kPa, 100 kPa and 200 kPa were carried out to determine the cohesion and friction angle in the triaxial apparatus. Figs. 9 and 10 show the variation of cohesion and friction angle under various applied voltages and concentrations of injected solution. The increase of applied voltage and the

*Int. J. Electrochem. Sci.,* 16 (**2021**) Article Number: 211215

12

concentration of chemical solution promoted the rate of ionic migration from the injected solution. Due to the inward diffusion of the salt into the slurry, the thickness of the double layer of soil particles decreased. It will result in the increase of van der Waals's attractive forces among the soil particles. While these processes increased the interparticle forces among the soil particles, they also led to the formation of aggregates of soil particles. The aggregates were coarser than the kaolin particles. Therefore, an increase in the shear strength and its parameters (cohesion and friction angle) was observed under higher applied voltage and concentration of injected solution. In addition, comparisons between Figures 9 and 10 indicated that the middle section exhibited higher cohesion and friction angle after the treatment. This means that the pozzolanic reaction (given by Equation (8)) occurred around the middle section.
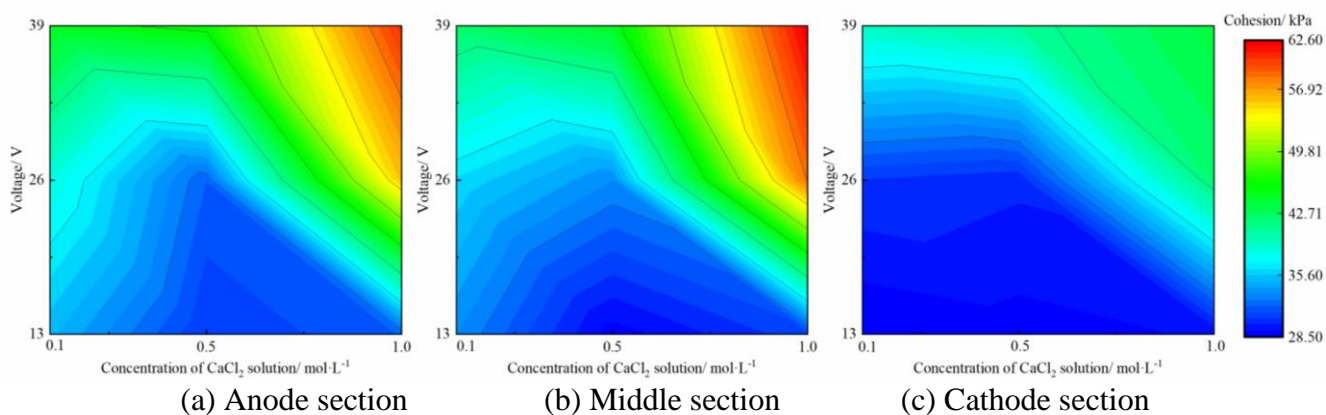


(a) Anode section        (b) Middle section        (c) Cathode section

**Figure 9**. Cohesion of the slurry after treatment



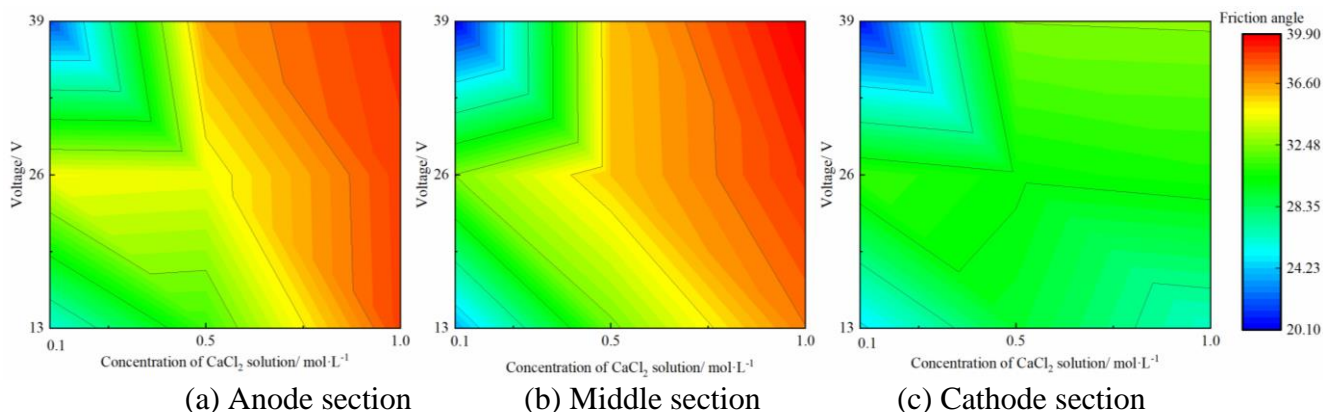(a) Anode section        (b) Middle section        (c) Cathode section

**Figure 10**. Friction angle of the slurry after treatment

In order to observe the variation of aggregate cluster formation after the electro-osmotic chemical treatment, the samples from anode, middle and cathode sections were collected to observe the microstructures using SEM. Figure 11 presents the SEM image for the untreated slurry. Figure 12 shows the photographs of the sample (EC_1.0_1.5) at the anode, middle and cathode sections after the treatment. Comparisons between the treated and untreated samples indicated that soil particles were

distributed more uniformly in the untreated slurry. On the contrary, soil particles in the treated samples were closely arranged and tended to form aggregates. In addition, some acicular material was generated during the electro-osmotic treatment at the middle section. The acicular material originated from the reaction products (as given by Equation (8)) and cemented the soil particles. The experimental data was consistent with the conclusion that C-S-H was formed in higher pH alkaline environment (Ou et al. [33]). The SEM results provide further evidence for the increase in shear strength and its parameters (cohesion and friction angle) , as shown in Figures 10, 11 and 12.
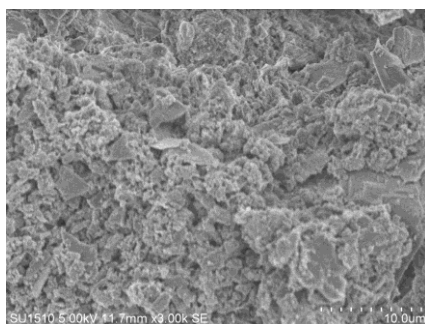


**Figure 11**. Soil fabric of untreated sample observed using scanning electron microscope
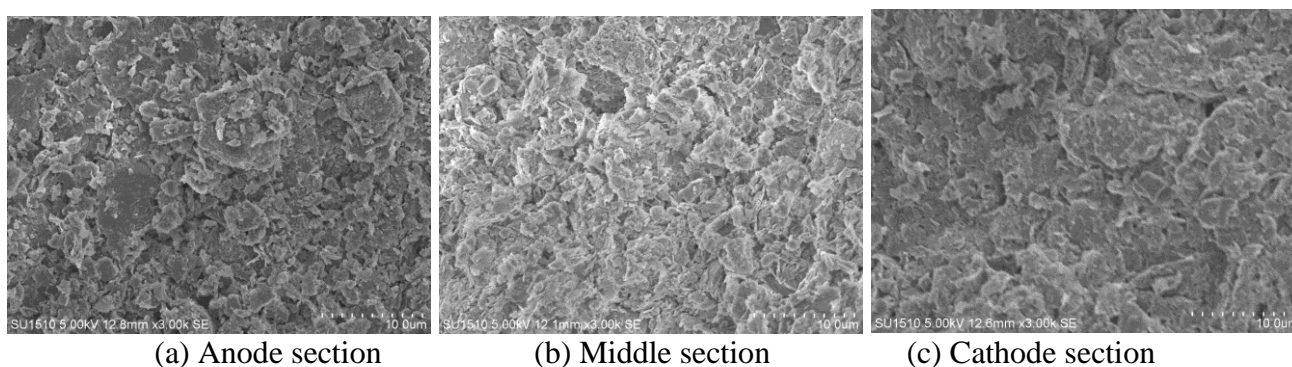


(a) Anode section          (b) Middle section          (c) Cathode section

**Figure 12**. Soil fabric of treated sample (EC_1.0_1.5) observed using scanning electron microscope

## 4. CONCLUSIONS

A series of electro-osmotic chemical experiments under different applied voltages and concentrations of chemical solution was conducted to assess the effectiveness and efficiency of the ECT. Based on the experimental results, following conclusions are drawn.

(1) The current, drainage volume, and settlement of the treated slurry sample were sensitive to applied voltage and concentration of injected solution, and increased with the increase in applied voltage and concentration of injected solution.

(2) The power consumption during the electro-osmotic treatment increased with the increase of applied voltage. It means that higher applied voltage reduced the economic effectiveness of ECT. However, the concentration of injected solution had little influence on the economic effectiveness of

ECT. The effectiveness and efficiency of ECT can be improved at lower applied voltages and higher concentrations of injected solution.

(3) ECT changed the microstructure of the sample was changed by the. This led to the variation in cohesion and friction angle of the treated sample. The value of the cohesion and friction angle of the treated sample increased with the applied voltage and the concentration of chemical solution.

CONFLICT OF INTEREST
On behalf of all authors, the corresponding author states that there is no conflict of interest.

DATA AVAILABILITY
The data used to support the findings of this study are available from the corresponding author upon request.

**References**

1. I. L. Casagrande, *Geotechnique*, 1 (1949) 159.
2. J. Lamont-Black, C. J .F. P. Jones, D. Alder, *Geotext. Geomembr.*, 44 (2016) 319.
3. J. Ling, B. Han, Y. Xie, Q. Dong, Y. Sun and B. Huang, *J. Cold Reg. Eng.*, 31 (2017) 04017010.
4. W. L. Zou, Y. F. Zhuang, X. Q. Wang, S. K. Vanapalli, Y. L. Huang and F. F. Liu, *Mar. Geores. Geotechnol.*, 36 (2017) 100.
5. C. Y. Ou, C. Shao and H. H. Chang, *Can. Geotech*. J., 46 (2009) 727.
6. L. Zhang, N. W. Wang, L. P. Jing, C. Fang, Z. D. Shan and Y. Q. Li, *Geotech. Test. J.*, 40 (2017) 72.
7. E. Mohamedelhassan and J. Q. Shang, *Can. Geotech. J.*, 40 (2003) 1185.
8. N. Otsuki, W. Yodsudjai and T. Nishida, *Constr. Build. Mater.*, 21 (2007) 1046.
9. H. A. Keykha, B. B. Huat and A. Asadi, *Geotech. Geol. Eng.*, 32 (2014) 739.
10. H. W. Chang, P. G. Krishna, S. C. Chien, C. Y. Ou and M. K. Wang, *Clays Clay Miner.*, 58 (2010) 154.
11. S. C. Chien, C. Y. Ou and Y. C. Lee, *Appl. Clay Sci.*, 50 (2010) 481.
12. Z. Xue, X. Tang, Q. Yang, Z. Tian, Y. Zhang and W. Xu, *Appl. Clay Sci.*, 166 (2018) 18.
13. F. Liu, H. Fu, J. Wang, W. Mi, Y. Cai and X. Geng, *Soil Mech. Found. Eng.*, 54 (2017) 49.
14. Z. Xue, X. Tang, Q. Yang, Z. Tian and Y. Zhang, *Dry. Technol.*, 37 (2019) 2015.
15. S. Gargano, S. Lirer, B. Liguori and A. Flora, *Soils Found.*, 60 (2020) 898.
16. F. Zhang, G. Wang, T. Kamai, W. Chen, D. Zhang and J. Yang, *Eng. Geol.*, 155 (2013) 69.
17. H. Wu and L. Hu, *Appl. Clay Sci.*, 101 (2014) 503-509.
18. C. Y. Ou, S. C. Chien and R. H. Liu, *Appl. Clay Sci.*, 104 (2015) 168.
19. V. A. Korolev and D. S. Nesterov, *J. Environ. Sci. Health Part A-Toxic*, 54 (2019) 570.
20. N. S. Nordin, S. A. Tajudin and A. A. Kadir, *Int. J. Zero Waste Gen.*, 1 (2013) 5.
21. S. C. Chien, F. C. Teng and C. Y. Ou, *Acta Geotech.*, 10 (2015) 813.
22. C. Cameselle and K. R. Reddy, *Electrochim. Acta,* 86 (2012) 10.
23. S. C. Chien, C. Y. Ou and M. K. Wang, *Appl. Clay Sci.,* 44 (2009) 218.
24. E. Mohamedelhassan and J. Q. Shang, *Proc. Inst. Civ. Eng. Ground Improv.*, 6 (2002) 145.
25. S. Gargano, S. Lirer and A. Flora, *Proc. Inst. Civ. Eng. Ground Improv.*, 172 (2019) 146.
26. K. Beddiar, T. Fen-Chong, A. Dupas, Y. Berthaud and P. Dangla, *Transp. Porous Media*, 61 (2005) 93.
27. A. Mahmoud, A. F. A. Hoadley, J. B. Conrardy, J. Olivier and J. Vaxelaire, *Water Res.*, 103 (2016)

    109.
28. A. Mahmoud, A. F. A. Hoadley, M. Citeau, J. M. Sorbet, G. Olivier, J. Vaxelaire and J. A. Olivier, *Water Res*., 129 (2018) 66.
29. C. Y. Ou, S. C. Chien and Y. G. Wang, *Appl. Clay Sci.,* 44 (2009) 130.
30. H. W. Chang, P. G. Krishna, S. C. Chien, C. Y. Ou and M. K. Wang, *Clays Clay Miner.*, 58 (2010) 154.
31. B. Tiwari, G. R. Tuladhar and H. Marui, *J. Geotech. Geoenviron. Eng*., 131 (2005) 1445.
32. M. Li, S. Chai, H. Du and C. Wang, *Soils Found*., 56 (2016) 327.
33. C. Y. Ou, S. C. Chien, C. C. Yang and C. T. Chen, *Appl. Clay Sci*., 104 (2015) 13.